

SUPPLEMENTARY INFORMATION

Mechanism of ribosome shutdown by RsfS in *Staphylococcus aureus* revealed by integrative structural biology approach

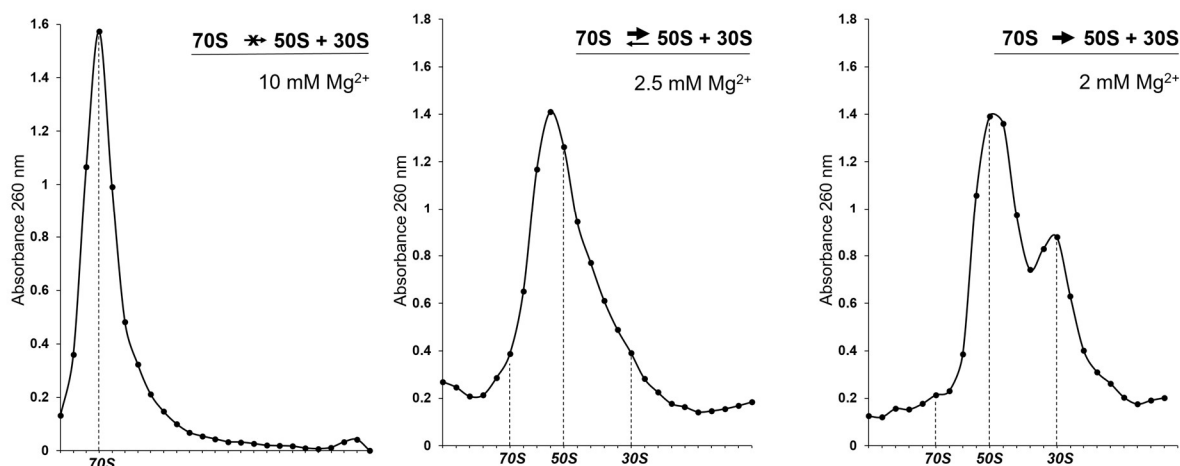
Khusainov et al.

Supplementary Figures 1 – 6

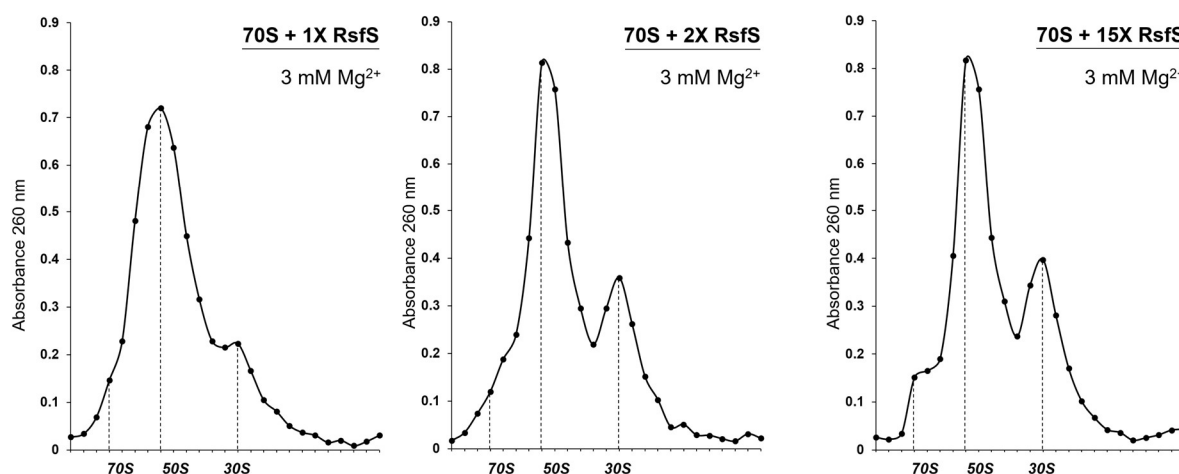
Supplementary Tables 1 – 3

SUPPLEMENTARY FIGURES

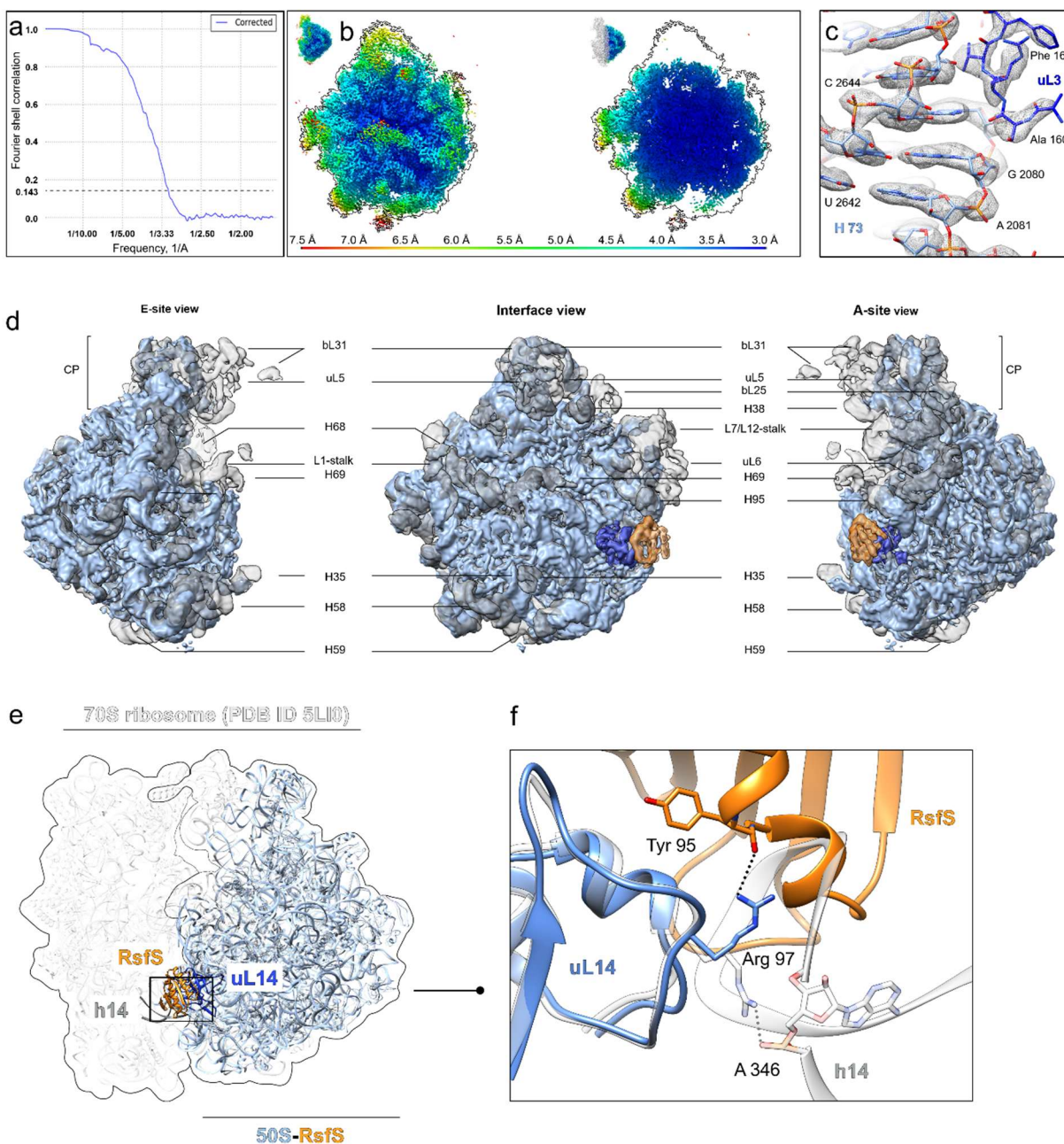
a The dynamic equilibrium 70S \leftrightarrow 50S + 30S is reached at 3 mM Mg^{2+}



b The anti-association activity of RsfS is reached at 2X molar excess



Supplementary Figure 1. Sucrose gradient (SG) profiles of the 70S and RsfS at semi-dissociation conditions. **a** Effect of magnesium on *S. aureus* ribosome subunits association. At 10 mM Mg^{2+} the 70S ribosomes remain intact (left panel); at 2.5 mM Mg^{2+} the ribosomes dissociate partly with the equilibrium shifted towards dissociation (middle panel); at 2 mM Mg^{2+} 70S ribosomes are fully dissociated into 30S and 50S individual subunits (right panel). **b** RsfS titration to determine the 70S:RsfS ratio sufficient to prevent ribosome re-association at 3 mM Mg^{2+} . At 1:1 ratio, the equilibrium is partly shifted towards dissociation (left panel), the maximum activity reached at 1:2 ratio (middle panel). Increasing RsfS to 15X molar excess did not significantly affect the profile further (right panel). Source data for Fig 1a-b and are provided as a Source Data file.



Supplementary Figure 2. Cryo-EM structure analysis of the 50S-RsfS complex. **a** Fourier Shell Correlation (FSC) curve indicating the overall resolution of the final 50S-RsfS reconstruction. **b** Local resolution (rainbow scale) displayed on representative slices of the density map for the 50S-RsfS complex. **c** The density and the model of 23S rRNA and uL3 protein in the core of the 50S. **d** Comparison of the cryo-EM density of the 50S-RsfS complex (current study, blue) and vacant 70S ribosome (PDB ID 5LI0 [<http://dx.doi.org/10.2210/pdb5LI0/pdb>]¹, grey). Both maps were Gaussian filtered with the width equal to 3.5 pixel size of the initial maps. In the absence of small subunit and potentially due to additional purification steps in low Mg²⁺ concentration, the periphery and the interface of the 50S became partly disordered or completely absent on the cryo-

EM map (regions have been labeled). Despite the overall disorder, uL14 (dark blue) and RsfS (orange) proteins had a high signal on the cryo-EM density map of the 50S-RsfS complex. For representation clarity, the density maps of the uL14 and RsfS were also coarsely segmented from the original map using Segger ² and Gaussian filtered with the width equal to 3.5 pixel size and colored accordingly. CP – central protuberance. **e** An overlay of 50S-RsfS complex (blue ribbon) on the vacant *S. aureus* 70S (faint grey ribbon). The binding site of RsfS (orange) would clash with the helix 14 (h14) of the 16S rRNA (dark grey), thus preventing 30S association. **f** A close-up view of the clashing region, where helix 14 and loop Met27 – Asp35 from RsfS would impede rearrangement of the rRNA upon joining of the 30S. More into details, the side chain of Arg97 of uL14 is interacting with the backbone of A346 of the 16S rRNA in the presence of the 30S or with the backbone of Tyr95 in RsfS.

a uL14

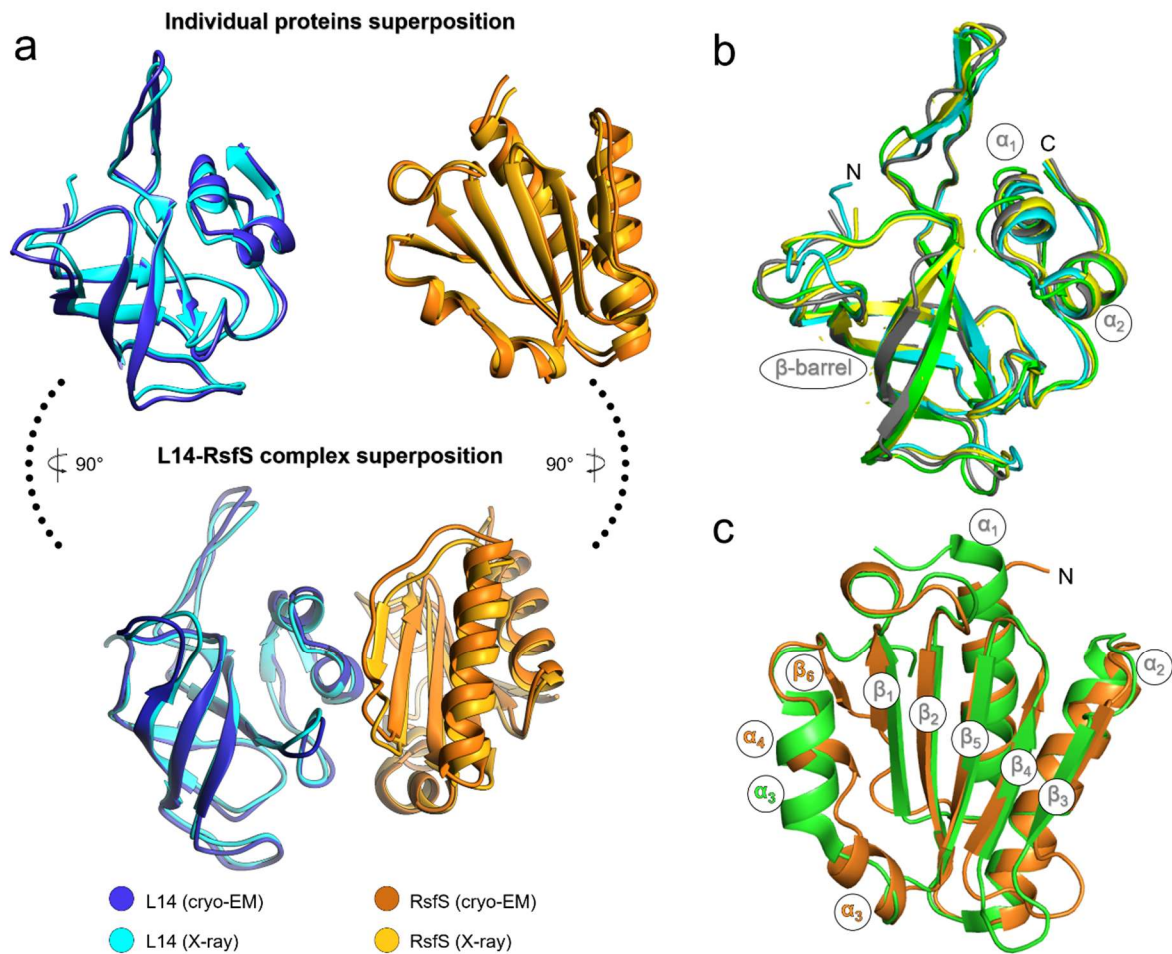
S.aureus	MIQQETRLKVADNSGAREVLTIKVLGGSSGRKTANIGDVIIVCTVKNATPGGVVKKGDVVK	60
B.subtilis	MIQQETRLKVADNSGAREVLTIKVLGGSSGRKTANIGDVIIVCTVKNATPGGVVKKGEVVK	60
L.monocytogenes	MIQQESRMKVADNSGAREVLTIKVLGGSSGRKTANIGDVIIVCTVKNATPGGVVKKGEVVK	60
E.faecalis	MIQQESRLRVADNSGAREILTIVLGGSSGRKTANIGDVIIVATVKQATPGGVVKKGEVVK	60
S.pneumoniae	MIQTETRLKVADNSGAREILTIVLGGSSGRKFANIGDVIIVASVKQATPGGAVKKGDVVK	60
S.iniae	MIQQETRLKVADNSGAREILTIVLGGSSGRKFANIGDVIIVASVKQATPGGAVKKGDVVK	60
A.flavithermus	MIQQETRMKVADNSGAREVLIVLGGSSGRRYANVGDIVVATVKQATPGGVVKKGQVVK	60
C.difficile	MIQQESRLRVADNSGAREILCIRVLGGSSGRRYGNIGDVIIVATVKSATPGGVVKKGKVVK	60
L.lactis	MIQTESRLKVADNSGARELLTIRVLGGSSSRKFAGIGDIVVATVKSAPGGAVKKGEVVK	60
M.tuberculosis	MIQQESRLKVADNTGAREILCIRVLGGSSSRRYAGIGDVIIVATVKDAIPGGNVKRGDVVK	60
H.influenzae	MIQEQTMLDVADNSGARSVMCIKVLGGSSHRRYAAGDIIKITVKEAIPRGKVKKGDVVK	60
E.coli	MIQEQTMLNVADNSGARRVMCIKVLGGSSHRRYAAGDIIKITVKEAIPRGKVKKGDVVK	60
T.thermophilus	MIQPQTYLEVADNTGARKIMCIRVLKGSNAKYATVGDVIIVASVKEAIPRGAVKEGDVVK	60
V.cholerae	MIQMOTMLDAADNSGARSVMCIKVLGGSSHRRYAAGDIIKVTVKEAIPRGKVKKGDVVK	60
P.aeruginosa	MIQTQSMLDVADNSGARRVMCIKVLGGSSHRRYAAGDIIKVTVKEAIPRGKVKKQVMTA	60

S.aureus	VIVRTKSGVRRNDGSYIKFDENACVIRIIR-DKGPGRGTRIFGPVARELREGNFMKIVSLAPEVL	122
B.subtilis	VIVRTKSGARRSDGSYISFDENACVIRIIR-DKSPRGTRIFGPVARELRENNFMKIVSLAPEVI	122
L.monocytogenes	VIVRTKSGARRQDGSYIKFDENACVIRIIR-DKSPRGTRIFGPVARELRENNFMKIVSLAPEVL	122
E.faecalis	VIVRTKSGARRADGSYIKFDENAAVIRIIR-DKSPRGTRIFGPVARELRENNFMKIVSLAPEVL	122
S.pneumoniae	VIVRTKSGARRADGSYIKFDENAAVIRIIR-DKTPRGTRIFGPVARELREGGFMKIVSLAPEVL	122
S.iniae	VIVRTKTGARRPDGSYIKFDENAAVIRIIR-DKTPRGTRIFGPVARELREGGFMKIVSLAPEVL	122
A.flavithermus	VIVRTKRGVRRDGSYIRFDENACVIRIIR-DKSPRGTRIFGPVARELREKDFMKIVSLAPEVI	122
C.difficile	VIVRTKQGMRRNDGSYISFDENAAVIRIIR-DKTPVGRTRIFGPVARELRDNEFMKIVSLAPEVL	122
L.lactis	VIVRTKSGAKRPDGSYIKFDENAAVIRIIR-DKTPRGTRIFGPVARELREGGFMKIVSLAPEVL	122
M.tuberculosis	VIVRTVKERRPDGSYIKFDENAAVIRIIR-DNDPRGTRIFGPVARELREKRFMKIVSLAPEVL	122
H.influenzae	VIVRTKKGVRPDGSVIRFDGNACVIRIIR-DNDPRGTRIFGPVARELREKRFMKIVSLAPEVL	123
E.coli	VIVRTKKGVRPDGSVIRFDGNACVIRIIR-DNDPRGTRIFGPVARELREKRFMKIVSLAPEVL	123
T.thermophilus	VIVRTKKEVKRPDGSVIRFDENAAVIRIIR-DNDPRGTRIFGPVARELREKRFMKIVSLAPEVL	122
V.cholerae	VIVRTKKGVRPDGSVIRFDGNACVIRIIR-DNDPRGTRIFGPVARELREKRFMKIVSLAPEVL	123
P.aeruginosa	VIVRTKHGVRPDGSVIRFDGNAAVIRIIR-DNDPRGTRIFGPVARELREKRFMKIVSLAPEVL	122

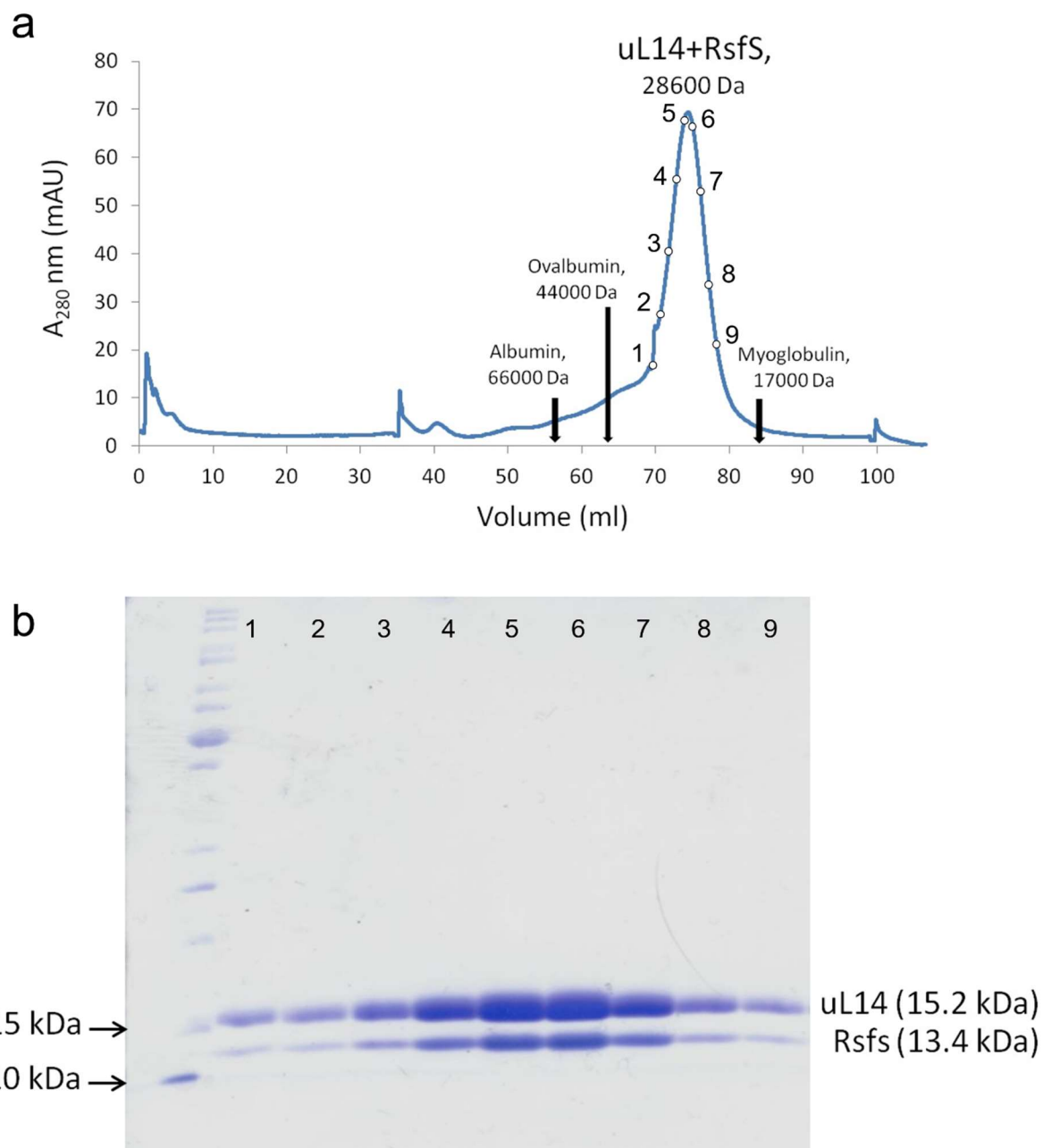
b RsfS

S.aureus	----MNSQELLAIIVDAIDNKKGEDTISLEMKGISDMDYFVVTHGNNERQVQAIARAVKEVAN	60
A.flavithermus	----MTERDILRIIVAADEKKAENIVALNMKGISLVADYFMICHGNSDKQVQAIAREIKEKAE	60
B.subtilis	----MNQKILKIAAAACDDKRAEDILALDMEGISLVADYFLICHGNSDKQVQAIAREIKQDAD	60
L.monocytogenes	----MNSYDTLMLTAKAADKRAEDILALDMKGLSFADYFVICHGNSDKQVQAIAREIKEKAL	60
E.faecalis	-----MLEIAVKAADSKRAEEIIVADVREISLLADYFLICQANSERQINAIIVDEINEQEA	55
S.iniae	----MKKEELLDIVVKAADKRAEDIIALNLEGLTSLTDYFVIATAGNTRQLEAIAENIREKVK	60
L.lactis	----MDSKKLLEVVKAAADKKAEDILALDMSEVTFVADYFVIMEAMNSRQLDAIADNIAEAAE	60
S.pneumoniae	----MNEKELLELVVKAADKRAEDILALDVQDLTSVTDYFVITSSMNSRQLDAIADNIREKVA	60
C.difficile	----MTVEQMTKIAYDAIEDKLQDVTIINIGKVSLLCDYFIITASSQRQVQAIADNVEDELA	60
E.coli	----MQGKALQDFVIDKIDDLKGGDIIVLDVQGGSSITDCMICTGTSSRHVMSIADHVQESR	60
M.tuberculosis	MTANREAIIDMARVAAGAAAKLADDVVIVDSGLVITDCFVIAAGSNERQVNAIIVDEVEEKMR	64
P.aeruginosa	----MQTEQLVQVAIDALEDLKAQDITVLDVDRKTSVTDYFVIAAGSSSRQVQKSLADNVLTAK	60
V.cholerae	----MQGEALKDFLFDKADDMKAVDITVLDVKEKSSVTDYFVIAAGSSSRQVQKSLADNVLTAK	60
H.influenzae	-----MALVEFLMETLDGLKGTIVHFDVGRKSSITDNMICTGTSSRQVSAMADNLITECK	57
T.thermophilus	MVKAKEAVALIERIKELLAEKKAENVVALDLRRVSETLOYFVVASATSTPHLQALERHLEKLE	64
S.aureus	EQNIE-VKRMGEYNEARWILIDLADVVHVHFKDERNYNIEKLYQDAPLESYGGQVLA----	117
A.flavithermus	EHDVV-VKRVGEFDEARWILVDLGDVVHVHFKDEREYNNLERLWGDAPLEQIESDLRA----	118
B.subtilis	ENGIQ-VKKMEGFDEARWILVDLGDVVHVHFKDERSYNNLEKLWGDAPLADLDLGMNQ----	118
L.monocytogenes	ENQVD-VKRLGEGFDEARWILVDLGDVVHVHFKDEERSYNNLEKLWGDAPLVDVSAAFIS----	118
E.faecalis	KNQVE-VKRVGEGEGGWILIDLGDVVHVHFKDEERSYNNLEKLWSDAPMVDLSAWVD----	112
S.iniae	EAGGD-ASHVEGDSVTGWILLDLNDVVHVFSEDERYHYNLEKLWHDAPVALNLDLA----	117
L.lactis	LAGAKAAGHIEGDAKTGWVILDLGDVVSVFVGHDERGHFNLEKLWSDAPMVDISGFMAE----	119
S.pneumoniae	QAGFK-GSHIEGDTGGWVILLDLGAVVVHIFSEEMRAHYNNLEKLWHEAHSVDLSETL-----	116
C.difficile	KLGLE-PRGKEGQGTQTVLLDYGDMVHVFEENRGFYNNLEKLWSDAPYIDIDTLA-----	116
E.coli	AAGLL-PLGVEGENSADWIVVDLGDVVHVHMQEESRRLYELEKLWS-----	105
M.tuberculosis	QAGYR-PARREGAREGRWILLDYRDIIVHIFHQDDRNFYALDRLWGDPCVVPVDLSANSAGAQ	126
P.aeruginosa	ENGVK-PLGSEGLESGEWALLDLGDVVHVHMLPATRQFYDLERLWQGAEQSRAHQHQP-----	118
V.cholerae	LSGLQ-PLGMNGENEGEWVLLDMGVSMLHVMQEAPELYQLEKLWG-----	105
H.influenzae	KAGFE-TFGEEGKNTADWIVVDLGAIVHIMQRDAREMYQLEKLWA-----	102
T.thermophilus	EEDLR-PRPTAG-QSPRWVLLDYGVEVVHMLTPEAREYYDLEGFWADAERL-----	113

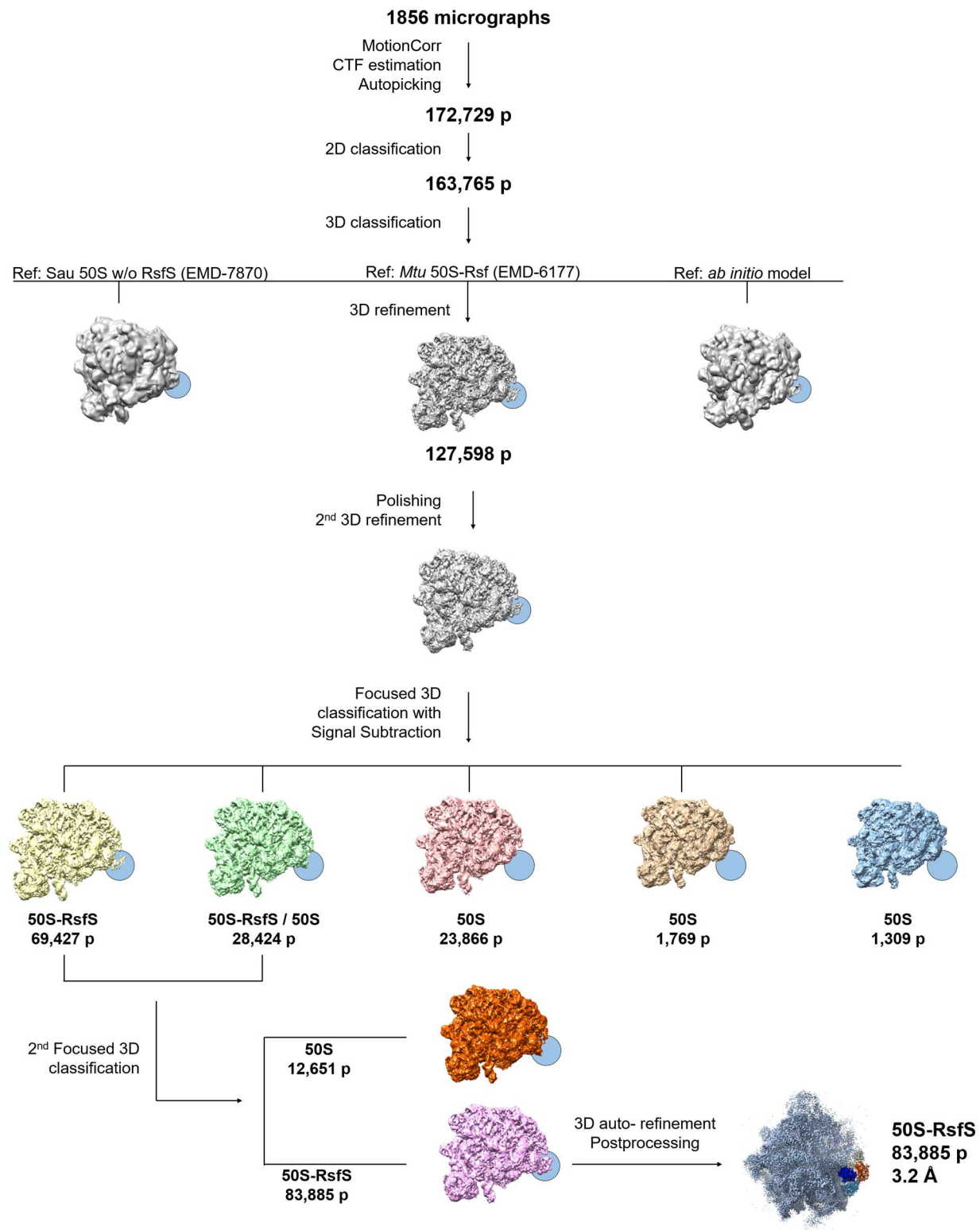
Supplementary Figure 3. Multiple sequence alignment of uL14 (panel **a**) and RsfS (panel **b**) proteins from 16 different bacterial species performed in Clustal Omega. Pink shading indicates positions that have a single, fully conserved residue (identity), yellow - conservation between amino acids with substantial chemical similarity and grey - amino acids with poor chemical similarity.



Supplementary Figure 4. Structural comparison of the uL14-RsfS complex within the 50S subunit solved by cryo-EM and crystal structure of the purified complex. **a** Superposition of individual proteins (upper part) and entire uL14-RsfS complex (lower part) derived from cryo-EM and the crystal structure. Color codes are indicated on the bottom of the figure panel. **b** Superposition of the crystal structure of uL14 from *S. aureus* (current study, cyan), *Geobacillus stearothermophilus* (PDB ID 1WHI [<http://dx.doi.org/10.2210/pdb1WHI/pdb>]³, grey), *Thermus thermophilus* (PDB ID 6N9E [<http://dx.doi.org/10.2210/pdb6N9E/pdb>]⁴, yellow) and *M. tuberculosis* (PDB ID 5V7Q [<http://dx.doi.org/10.2210/pdb5V7Q/pdb>]⁵, green). **c** Superposition of *S. aureus* RsfS crystal structure (current study, orange) and RsfS from *M. tuberculosis* (PDB ID 4WCW [<http://dx.doi.org/10.2210/pdb4WCW/pdb>]⁶, green). Grey labels of the secondary structure represent common elements, and colored labels represent species-specific features.



Supplementary Figure 5. Purification of the *S. aureus* uL14-RsfS complex for crystallization. **a** Size exclusion chromatography profile of the uL14-RsfS complex performed on a HiLoad 16/600 Superdex 75 prep grade column. Arrows indicate the positions of the molecular weight of reference proteins according to the manufacturer's calibration. The fractions that were taken for polyacrylamide gel electrophoresis (PAGE) are marked as white dots (1 to 9). **b** Analysis of the selected fractions by 15% PAGE. Fraction labels correspond to those in panel a).



Supplementary Figure 6. Cryo-EM 3D particles sorting. The total number of particles (p) used for the 3D reconstructions is indicated below each structure. Blue circles point to the localization of RsfS on the 50S. Coloring of the final map is the same as in Fig. 2a.

SUPPLEMENTARY TABLES

Supplementary Table 1. Mass spectrometry analysis of the 50S-RsfS complex used for cryo-EM structure determination.

Accession	Gene	Description	Modifications	SAF
P0A0F8	rplO	50S ribosomal protein uL15	Met-loss [N-Term]	2.77
P0A0G2	rpmD	50S ribosomal protein uL30	Met-loss [N-Term]	2.58
Q2FXS8	rplU	50S ribosomal protein bL21	Met-loss [N-Term]	2.30
P60430	rplB	50S ribosomal protein uL2		1.89
Q2FW38	rplM	50S ribosomal protein uL13	Met-loss [N-Term]	1.88
Q2FW18	rplE	50S ribosomal protein uL5		1.87
Q2FW06	rplC	50S ribosomal protein uL3		1.82
Q2FW11	rplV	50S ribosomal protein uL22		1.65
Q2FW33	rplQ	50S ribosomal protein bL17		1.53
Q2FW08	rplW	50S ribosomal protein uL23		1.33
Q2G0P0	rplA	50S ribosomal protein uL1		1.12
Q2FW21	rplF	50S ribosomal protein uL6		1.09
Q2G298	rsfS	Ribosomal silencing factor RsfS		1.07
Q2FW14	rpmC	50S ribosomal protein uL29		1.00
Q2FW29	rpmJ	50S ribosomal protein bL36		0.97
Q2FZ60	rpmB	50S ribosomal protein bL28		0.95
Q2FZ42	rplS	50S ribosomal protein bL19		0.87
Q2FWD8	rpmE2	50S ribosomal protein bL31 type B		0.83
Q2FW07	rplD	50S ribosomal protein uL4	Met-loss [N-Term]	0.77
Q2FXQ1	rplT	50S ribosomal protein bL20		0.75
Q2FW22	rplR	50S ribosomal protein uL18		0.71
Q2FXT0	rpmA	50S ribosomal protein bL27		0.66
Q2G0S0	rplY	50S ribosomal protein bL25		0.66
Q2G0N9	rplJ	50S ribosomal protein uL10		0.56
Q2FW16	rplN	50S ribosomal protein uL14		0.55
Q2FW17	rplX	50S ribosomal protein uL24		0.50
Q2FY22	rpmG2	50S ribosomal protein bL33 2		0.39
P0A0F4	rplK	50S ribosomal protein uL11		0.39
Q2FW31	rpsK	30S ribosomal protein uS11		0.28
Q2FW13	rplP	50S ribosomal protein uL16		0.27
Q2FXQ0	rpmI	50S ribosomal protein bL35		0.24
Q2FXZ7	rpsU	30S ribosomal protein bS21		0.24
Q2FW10	rpsS	30S ribosomal protein uS19		0.21
Q2G113	rpsF	30S ribosomal protein bS6		0.18
P48940	rpsG	30S ribosomal protein uS7		0.17
Q2FZ25	rpsB	30S ribosomal protein uS2		0.16
Q2FXK6	rpsD	30S ribosomal protein uS4		0.13
Q2FW12	rpsC	30S ribosomal protein uS3		0.10
Q2FW23	rpsE	30S ribosomal protein uS5		0.10
Q2FZ45	rpsP	30S ribosomal protein bS16		0.08

Q2G2A4	SAOUHSC_01042	Dihydrolipoamide acetyltransferase component of pyruvate dehydrogenase complex		0.08
Q2FXY2	SAOUHSC_01698	Uncharacterized protein		0.07
Q2G2A5	SAOUHSC_01041	Pyruvate dehydrogenase complex, E1 component, pyruvate dehydrogenase beta subunit, putative	Met-loss [N-Term]	0.07
Q2FW15	rpsQ	30S ribosomal protein S17		
Q2FZG4	SAOUHSC_01040	Pyruvate dehydrogenase complex, E1 component, alpha subunit, putative		0.07
Q2FW20	rpsH	30S ribosomal protein uS8	Met-loss [N-Term]	0.06
P0A0H0	rpsL	30S ribosomal protein uS12	Met-loss [N-Term]	0.05
Q2FW30	rpsM	30S ribosomal protein uS13		0.04
Q2FW39	rpsI	30S ribosomal protein uS9		0.03
P02976	spa	Immunoglobulin G-binding protein A		0.02
P0CE47	tufA	Elongation factor Tu 1 E. coli (K12)		0.02

Protein identification was performed from liquid sample. Proteins ranking is based on SAF (Spectrum Abundance Factor), from the most abundant to the less abundant. Components of the 50S subunit r-proteins and RsfS are shown in bold.

Supplementary Table 2. Potential hydrogen bonds between uL14 and RsfS in the two heterodimers of the unit cell in the crystal structure.

Contact atoms				Distance (Å)	
uL14	Conservation	RsfS	Conservation	Heterodimer 1	Heterodimer 2
Arg 107[NH1]	***	Met 33[O]	*	2.89	2.91
Arg 107[O]	***	Arg 68[NH1]		3.01	-
Asn 110[OD1]		Arg 68[NH1]		3.25	-
Met 112[N]	***	Glu 70[OE2]		2.57	2.88
Lys 113[N]	***	Glu 70[OE1]		3.05	3.08
Lys 113[NZ]	***	Trp 77[O]	***	2.51	2.75
Arg 107[NH2]	***	Asp 81[OD1]	***	2.54	2.30
Arg 107[NE]	***	Asp 81[OD2]	***	2.35	2.42
Arg 107[NH2]	***	Ala83[O]		3.17	3.31
Arg 97[NH1]	***	Tyr 98[O]	**	2.74	3.00
Arg 97[NH2]	***	Tyr 98[O]	**	2.85	2.69
Ser 116[O]	***	Tyr 104[OH]	**	2.50	2.72
Contacts mediated by water molecules					
Asp 90[OD2]		Trp 77[N]	***		
Pro 93 [O]	***	Tyr 98[OH]	**		

Asterisks define the conservation of these amino acids between 16 analyzed species presented in Supplementary Fig. 3 a,b (*** – identical (100%), ** – high conservative (>50%), * – low conservative (<50%), space – non-conserved amino acids).

Supplementary Table 3. Hydrophobic interactions (< 5 Å) between uL14 and RsfS in the two heterodimers of the unit cell in the crystal structure.

Contact amino acids					
uL14	Conservation	RsfS	Conservation	Heterodimer 1	Heterodimer 2
Met 112	***		*	+	+
Val 115	**	Met 33		+	+
Val 121	***			+	+
Met 112	***	Phe 37	**	-	+
Pro 93	***	Trp 77	***	+	+
Leu 117	***			+	+
Met 112	***	Leu 79	**	+	+
		Val 86	**	+	+
Pro 93	***	Tyr 98	**	-	+
Leu 117	***			+	+
Leu 117	***	Ile 100	**	+	+
Leu 117	***	Leu 103	**	+	+

Asterisks define the conservation of these amino acids between 16 analyzed species presented in Supplementary Fig. 3 a,b (*** – identical (100%), ** – high conservative (>50%), * – low conservative (<50%), space – non-conserved amino acids).

SUPPLEMENTARY REFERENCES

1. Khusainov, I. *et al.* Structure of the 70S ribosome from human pathogen *Staphylococcus aureus*. *Nucleic Acids Res.* **44**, gkw933 (2016).
2. Pintilie, G. D., Zhang, J., Goddard, T. D., Chiu, W. & Gossard, D. C. Quantitative analysis of cryo-EM density map segmentation by watershed and scale-space filtering, and fitting of structures by alignment to regions. *J. Struct. Biol.* **170**, 427–438 (2010).
3. Davies, C., White, S. W. & Ramakrishnan, V. The crystal structure of ribosomal protein L14 reveals an important organizational component of the translational apparatus. *Structure* **4**, 55–66 (1996).
4. Melnikov, S. V. *et al.* Mechanistic insights into the slow peptide bond formation with D-amino acids in the ribosomal active site. *Nucleic Acids Res.* (2019). doi:10.1093/nar/gky1211
5. Yang, K. *et al.* Structural insights into species-specific features of the ribosome from the human pathogen *Mycobacterium tuberculosis*. *Nucleic Acids Res.* **45**, 10884–10894 (2017).
6. Li, X. *et al.* Structure of Ribosomal Silencing Factor Bound to *Mycobacterium tuberculosis* Ribosome. *Structure* **23**, 1858–1865 (2015).